

Combustion and Emission Characteristics of SI Engines under Special Stroke/Bore Ratios

İsmet Sezer^{*1}, Yiğit Serkan Şahin²

^{1,2} Mechanical Engineering Department/Faculty of Engineering and Natural Sciences, Gümüşhane University, Turkey

Email of corresponding author: isezer@gumushane.edu.tr

(Received: 07 March 2024, Accepted: 12 March 2024)

(4th International Conference on Innovative Academic Studies ICIAS 2024, March 12-13, 2024)

ATIF/REFERENCE: Sezer, İ. & Şahin, Y. S. (2024). Combustion and Emission Characteristics of SI Engines under Special Stroke/Bore Ratios. *International Journal of Advanced Natural Sciences and Engineering Researches*, 8(2), 333-338.

Abstract – Effects of stroke to bore ratio (r_{sb}) on combustion and emission characters of spark ignited (SI) engines are investigated numerically in this work. With the intention of achieving this goal, two–zone quasi–dimensional cycle model for the SI engines was used, omitting detailed computation of the fluid dynamics. Using empirical correlations, thermodynamic characteristics during the suction and exhaust periods are estimated. SI cycle model's turbulent flame entrainment model was used to imitate the combustion phenomena, allowing for determination of combustion's properties, including temperature, cylinder pressure, burnt mass fraction, delay period, and duration. To look into the emission characteristics of the SI engines, the cycle model was also used to compute emissions for instance carbon monoxide (CO), nitrogen oxide (NO), and carbon dioxide (CO₂). Based on the study's findings, the characteristics of combustion and emissions were significantly impacted by adjusting the r_{sb} ratio. With a rising r_{sb} , the cylinder pressure and temperature rose along with a reduced ignition delay and combustion duration. There was a decrease of approximately 29.2% and 37.5% in the ignition delay and combustion time, respectively, when the r_{sb} rose from 0.7 to 1.3. Contrarily, CO and NO emissions dropped while CO₂ emissions remained mostly same as the stroke to bore ratio rose. When the r_{sb} rose from 0.7 to 1.3, CO and NO emissions decreased by almost 41% and 52.8%, respectively.

Keywords- Spark Ignition Engine, Cycle Model, Stroke To Bore Ratio, Combustion, Emissions

I. INTRODUCTION

Internal combustion engines (ICEs) are designed and operated to maximize output based on fuel qualities. This is accomplished by optimizing both the operational and design parameters. The results of the experimental and numerical studies showed that the emissions, heat release, cylinder pressure and temperature, rise of max pressure, and combustion duration are all significantly influenced by changes in the operating conditions, such as engine rpm, air–fuel ratio, combustion duration, valve overlap period, and residual gas rate [1]. Electronic control units (ECUs) have made it possible to adjust operating conditions appropriately in recent times. This has allowed for the application of design parameter flexibility with modified engine designs, such as variable valve timing, variable stroke length, variable compression ratio, and air boosting systems [2].

Additionally, geometry of combustion chamber, sizes of intake and exhaust ports, cam profile, valve design, position of spark plug, compression ratio, stroke to bore ratio (r_{sb}), and other design elements affect how well an ICE performs, burns fuel, and emits pollutants. To investigate effect of the design factors on engine outputs, a number of experiments were conducted [3–7]. To ascertain the engine characteristics, thermodynamic (zero– or quasi–dimensional) engine cycle models were extensively employed in the majority of these investigations. The cycle simulation models’ ability to find new designs before producing a prototype and running engine tests makes them realistic [2]. The purpose of this article is to look at how the r_{sb} affects SI engine emissions and combustion.

II. CYCLE MODEL

This work has employed a quasi–dimensional thermodynamic cycle model, which is mostly based on Ferguson’s [8] model. For the utilized model, original model’s equations were rearranged. By supposing that cylinder content complies with ideal gas law, cycle model’s governing equations were obtained from the energy equation, or first law of thermodynamics. As is commonly known, four periods of a spark ignition engine cycle are induction, compression, expansion, and exhaust. Approximation approach proposed by Bayraktar and Durgun [9] is used to compute the thermodynamic parameters of the gases during induction and exhaust. Pressure loss throughout induction is computed using Bernoulli equation for one–dimensional incompressible flow in this technique. As a result, temperature and pressure of fuel–air mixture of fresh charge are defined as follow.

$$p_{int} = p_0 - \Delta p_{ind} \quad (1)$$

$$T_{int} = \frac{(T_0 + \Delta T_{ind} + r_{rg} T_{exh})}{(1 + r_{rg} T_{exh})} \quad (2)$$

Where; p_0 and T_0 are surrounding pressure and temperature. Δp_{int} is pressure loss along with induction system and ΔT_{int} is variation in temperature of fresh charge.

The volumetric efficiency is defined as follow.

$$\eta_v = \gamma_{abc} \left(\frac{r_{comp}}{r_{comp} - 1} \right) \left(\frac{p_{ind}}{p_0} \right) \left(\frac{T_0}{T_0 + \Delta T + r_{rg} T_{exh}} \right) \quad (3)$$

Where; γ_{abc} is the air boosting coefficient and r_{rg} is molar ratio of residual gases.

Appropriate arrangement of cycle governing equations for each period allows computation of compression, combustion, and expansion periods. Following equations are used to compute the exhaust gas pressure (p_{exh}) and temperature (T_{exh}), which rely on ambient pressure (p_0) and temperature of burnt gas (T_b).

$$p_{exh} = (1.05 \approx 1.25) p_0 \quad (4)$$

$$T_{exh} = \frac{T_b}{(p_b / p_{exh})^{1/3}} \quad (5)$$

References [10, 11] contain all of the cycle model’s information.

III. NUMERICAL APPLICATIONS

For the cycle model that is being presented, computer code has been built. The software took as input parameters r_{comp} , n , ϕ , r_{sp} , θ_{st} , fuel characteristics, surrounding pressure and temperature. Solving governing differential equations allows one to forecast thermodynamic state of cylinder charge once intake circumstances were established. DVERK subroutine is used to integrate these differential equations. FARG (fuel–air–residual gas) and ECP (equilibrium–combustion–products), FORTRAN subroutines that were first created by Ferguson [8], determine composition and thermodynamic characteristics of cylinder content in simulation. In cycle simulation, acquired findings are finally adjusted as error analysis follows [8, 10].

$$\varepsilon_1 = 1 - \left(\frac{vm}{V} \right) \quad (6)$$

$$\varepsilon_2 = 1 + \left[\frac{W}{\Delta(m e_{int})} + Q_{cw} \right] \quad (7)$$

By setting values of ε_1 and ε_2 to 10^{-4} , assurance of cycle simulation program is fulfilled.

IV. RESULTS AND DISCUSSION

Predicted values for conditions shown on Fig. 1(a) and (b) and engine characteristics listed in Table 1 are checked with experimental data to show reliability of cycle model that is being presented.

Table 1. Dimensions of engines used for comparison

Specification	r_{comp}	r_{sp}	D_c [mm]	L_s [mm]	L_{cr} [mm]	D_{iv} [mm]	$L_{iv,max}$ [mm]
Engine I [12]	7	0.1	76.2	111.1	220	30	4.2
Engine II [13]	5	0.3	63.5	76.2	127	25	4.8

Estimate of cylinder pressure and mass fraction burnt using cycle model is in good conformity by experimental data as seen from figures. Thus, developed cycle model may be considered sufficiently confident for parametric and performance investigation.

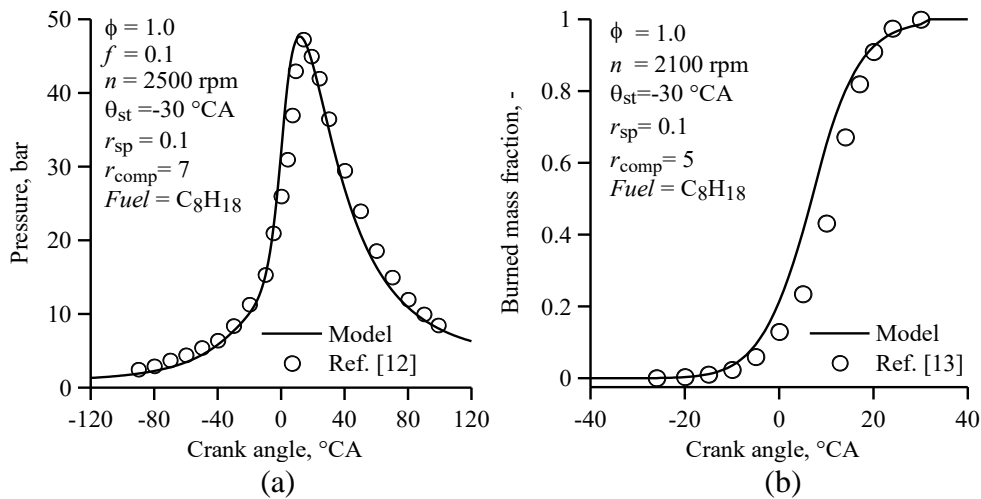


Fig. 1. Comparison of the model values with experimental data

This study has examined three distinct cylinders with varying r_{sb} and same displacement volume (400 cm^3). Values of r_{sb} seen in Table 2 were used as in Ref. [5].

Table 2. Engine dimensions for parametric study [5]

r_{sb}	0.7	1.0	1.3
L_s , mm	62.8	79.5	95.5
D_c , mm	90	80	73
L_{cr} , mm	126	159	191
r_{comp}	9	9	9
D_{iv} , mm	39.4	35	32
$L_{iv,max}$, mm	5.74	8.95	8.17
V_d , cm^3	400	400	400
θ_d , °CA	24	16	10
θ_b , °CA	99	72	62

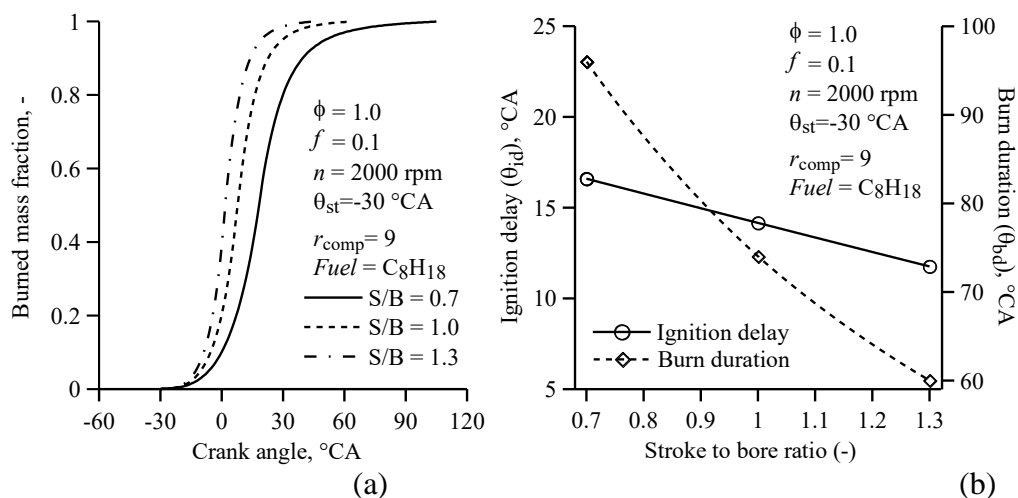


Fig. 2. Effect of r_{sb} on a) burned mass fraction and b) ignition delay and combustion duration

Figure 2(a) illustrates how the mass fraction burned varies with crank angle for selected r_{sb} under conditions specified on figure. As seen in Fig. 2(a), burned mass fraction increases with increasing r_{sb} due to reduction of ignition delay and burn duration as seen in Fig. 2(b). Fig. 3(a) and (b) show variation of cylinder pressure, unburned and burned gas temperature with crank angle for selected r_{sb} for conditions specified on the figure. As seen in Fig. 3(a), cylinder pressure and temperature increase earlier with increasing r_{sb} . Moreover, cylinder pressure and temperature increase earlier with increase of r_{sb} due to reduced ignition delay and completion of combustion in shorter time.

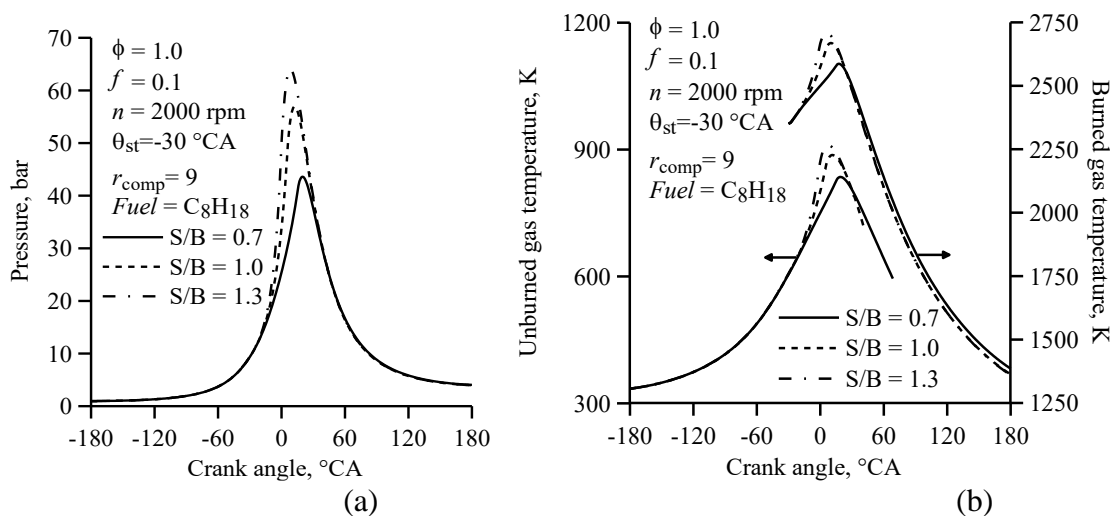
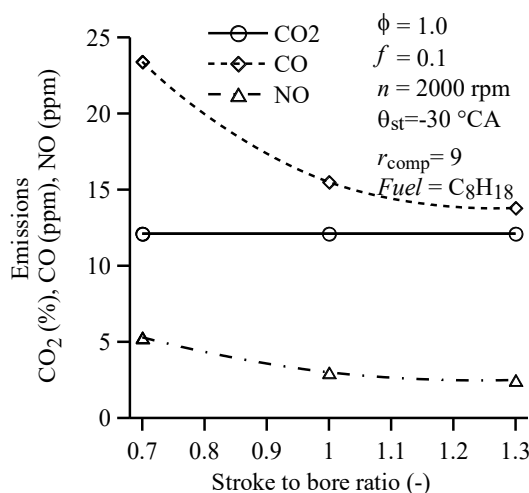


Fig. 3. Effect of r_{sb} on a) pressure b) unburned and burned gas temperature

Fig. 4 shows variation of CO_2 , CO and NO emissions with selected r_{sb} for conditions specified on Fig. 4. As seen in Fig. 4, CO_2 emission is almost stable for all r_{sb} . This sourced from the volume of cylinder does not change with r_{sb} ; hence the sending of fuel–air mixture into cylinder is about same for all r_{sb} . From the figure, CO and NO emissions reduce with increase of r_{sb} . The shortened combustion duration prevent the deterioration of combustion reactions, thus CO and NO emissions reduce with the increasing r_{sb} .

Fig. 4. Effect of r_{sb} on CO₂, CO and NO emissions

V. CONCLUSIONS

This paper investigates numerically effects of stroke to bore ratio (r_{sb}) on combustion and emissions. Following conclusions were summed up from the findings.

- Ignition delay and combustion duration decrease, but cylinder pressure and temperature increase with rise of r_{sb} . Ignition delay is lower %14.7 and 29.2% for r_{sb} of 1 and 1.3 compared to r_{sb} of 0.7. The combustion duration is shorter %23 and %37.5 for stroke r_{sb} of 1 and 1.3 compared to r_{sb} of 0.7.
- The CO and NO emissions reduce, while CO₂ emissions stay almost stable with the increase of r_{sb} . CO emission is lower %33.7 and 41% for r_{sb} of 1 and 1.3 compared to r_{sb} of 0.7. NO emission is less %43.4 and %52.8 for stroke to bore ratio of 1 and 1.3 compared to r_{sb} of 0.7.
- Consequently, it can be said that the increase of r_{sb} reduced at the certain level reduces the emissions by improving the combustion.

ABBREVIATIONS

°CA	: degree crank angle
CO	: carbon monoxide
CO ₂	: carbon dioxide
ECU	: electronic control unit
ICE	: internal combustion engine
NO	: nitrogen oxide
SI	: spark ignition

NOMENCLATURE

D_c	: diameter (bore) of cylinder, m
D_{iv}	: intake valve diameter, m
e_{int}	: specific internal energy, J/kg
f	: residual gas mass fraction, dimensionless
L_{cr}	: connecting rod length, m
$L_{iv, max}$: maximum intake valve lift, m
L_s	: stroke length, m
m	: mass, kg
n	: engine speed, rpm
p	: pressure, bar
Q_{cw}	: total heat transfer from the cylinder wall, J
r_{comp}	: compression ratio, dimensionless

r_{rg}	: residual gas molar ratio, dimensionless
r_{sb}	: stroke to bore ratio, dimensionless
r_{sp}	: spark plug location ratio, dimensionless
T	: absolute temperature, K
v	: specific volume, m ³ /kg
V	: volume, m ³
V_c	: volume of combustion chamber, m ³

GREEK LETTERS

ε	: error ratio, dimensionless
ϕ	: fuel–air equivalence ratio, dimensionless
γ_{abc}	: air boosting coefficient
η_v	: volumetric efficiency, %
θ	: crank angle, °CA
θ_{bd}	: burn (combustion) duration, °CA
θ_{id}	: ignition delay, °CA
θ_{st}	: spark timing crank angle, °CA

REFERENCES

- [1] N. X. Khoa, Q. Nhu and O. Lim, (2020). Estimation of parameters affected in internal exhaust residual gases recirculation and the influence of exhaust residual gas on performance and emission of a spark ignition engine. *Applied Energy*, 278, Paper no 115699.
- [2] H. Ozcan and J. A. A. Yamin, (2008). Performance and emission characteristics of LPG powered four stroke SI engine under variable stroke length and compression ratio. *Energy Conversion and Management*, 49, 1193–1201.
- [3] S. G. Poulos and J. B. Heywood, (1983). The effect of chamber shape on spark ignition engine combustion. *Society of Automotive Engineering*, Paper no 830334, 1–27.
- [4] N. W. Sung and S. P. Jun, (1997). The effects of combustion chamber geometry in an SI engine. *Society of Automotive Engineering*, Paper no 972996, 227–239.
- [5] Z. S. Filipi and D. N. Assanis, (2000). The effect of the stroke–to–bore ratio on combustion, heat transfer and efficiency of a homogeneous charge spark ignition engine of given displacement. *International Journal of Engine Research*, 1(2), 191–208.
- [6] E. Sher and T. Bar–Kohany, (2002). Optimization of variable valve timing for maximizing performance of an unthrottled SI engine—a theoretical study. *Energy*, 27, 757–775.
- [7] Z. Hu, J. H. Whitelaw and C. Vafidis, (1992). Flame propagation studies in a four–valve pentroof–chamber spark ignition engine. *Society of Automotive Engineering*, Paper no 922321, 1–11.
- [8] C. R. Ferguson, *Internal combustion engine, applied thermosciences*, New York: John Wiley & Sons Inc., 1985.
- [9] H. Bayraktar and O. Durgun, (2003). Mathematical modeling of spark–ignition engine cycles. *Energy Sources*, 25, 651–666.
- [10] I. Sezer, *Application of exergy analysis to spark ignition engine cycle*, PhD Dissertation, Blacksea Technical University, Trabzon–Turkey, 2008.
- [11] I. Sezer, (2023). Effects of stroke to bore ratio on exergy balance in spark ignition engines. *International Journal of Automotive Engineering and Technologies*, 12(1), 30–43.
- [12] C. D. Rakopoulos, (1993). Evaluation of a spark ignition engine cycle using first and second law analysis techniques. *Energy Conversion and Management*, 34(12), 1299–1314.
- [13] N. C. Blizard and J. C. Keck, (1974). Experimental and theoretical investigation of turbulent burning model for internal combustion engines. *Society of Automotive Engineers*, Paper no 740191, 846–864.